Biology of Reproduction, 2020, 103(5), 951–965
doi:10.1093/biolre/ioaa143
Research Article
Advance Access Publication Date: 23 August 2020

Research Article

Increased FOXL2 expression alters uterine structures and functions†

Rong Li[1], San-Pin Wu[1], Lecong Zhou[2], Barbara Nicol[1], John P. Lydon[3], Humphrey H-C Yao[1] and Francesco J. DeMayo[1,*]

[1]Reproductive and Developmental Biology Laboratory, National Institute of Environmental Health Sciences, Research Triangle Park, NC, USA, [2]Integrative Bioinformatics, National Institute of Environmental Health Sciences, Research Triangle Park, NC, USA and [3]Department of Molecular and Cellular Biology, Baylor College of Medicine, Houston, TX, USA

***Correspondence**: Reproductive and Developmental Biology Laboratory, National Institute of Environmental Health Sciences, 111 T. W. Alexander Dr., Research Triangle Park, NC 27709, USA. Tel: (984) 287-3987;
E-mail: demayofj@niehs.nih.gov

†**Grant support:** This work was funded by an Intramural Research Program of the National Institute of Health (NIH) Z1AES103311-01 to F.J.D. and a NIH/National Institute of Child Health and Human Development RO1 HD042311 to J.P.L.

Received 9 March 2020; Revised 29 June 2020; Accepted 10 August 2020

Abstract

The transcription factor forkhead box L2 (FOXL2) regulates sex differentiation and reproductive function. Elevated levels of this transcription factor have been observed in the diseases of the uterus, such as endometriosis. However, the impact of elevated FOXL2 expression on uterine physiology remains unknown. In order to determine the consequences of altered FOXL2 in the female reproductive axis, we generated mice with over-expression of FOXL2 ($FOXL2^{OE}$) by crossing *Foxl2*$^{LsL/+}$ with the *Progesterone receptor Pgr*^{cre} model. $FOXL2^{OE}$ uterus showed severe morphological abnormality including abnormal epithelial stratification, blunted adenogenesis, increased endometrial fibrosis, and disrupted myometrial morphology. In contrast, increasing FOXL2 levels specifically in uterine epithelium by crossing the *Foxl2*$^{LsL/+}$ with the *lactoferrin Ltf*^{icre} mice resulted in the $eFOXL2^{OE}$ mice with uterine epithelial stratification but without defects in endometrial fibrosis and adenogenesis, demonstrating a role of the endometrial stroma in the uterine abnormalities of the $FOXL2^{OE}$ mice. Transcriptomic analysis of 12 weeks old *Pgr*^{cre} and $FOXL2^{OE}$ uterus at diestrus stage showed multiple signaling pathways related with cellular matrix, wnt/β-catenin, and altered cell cycle. Furthermore, we found $FOXL2^{OE}$ mice were sterile. The infertility was caused in part by a disruption of the hypophyseal ovarian axis resulting in an anovulatory phenotype. The $FOXL2^{OE}$ mice failed to show decidual responses during artificial decidualization in ovariectomized mice demonstrating the uterine contribution to the infertility phenotype. These data support that aberrantly increased FOXL2 expressions in the female reproductive tract can disrupt ovarian and uterine functions.

Summary Sentence

FOXL2 overexpression in the uterus induced epithelial stratification, blunted adenogenesis, increased fibrosis, and disrupted myometrium leading to impaired decidual responses.

Graphical Abstract

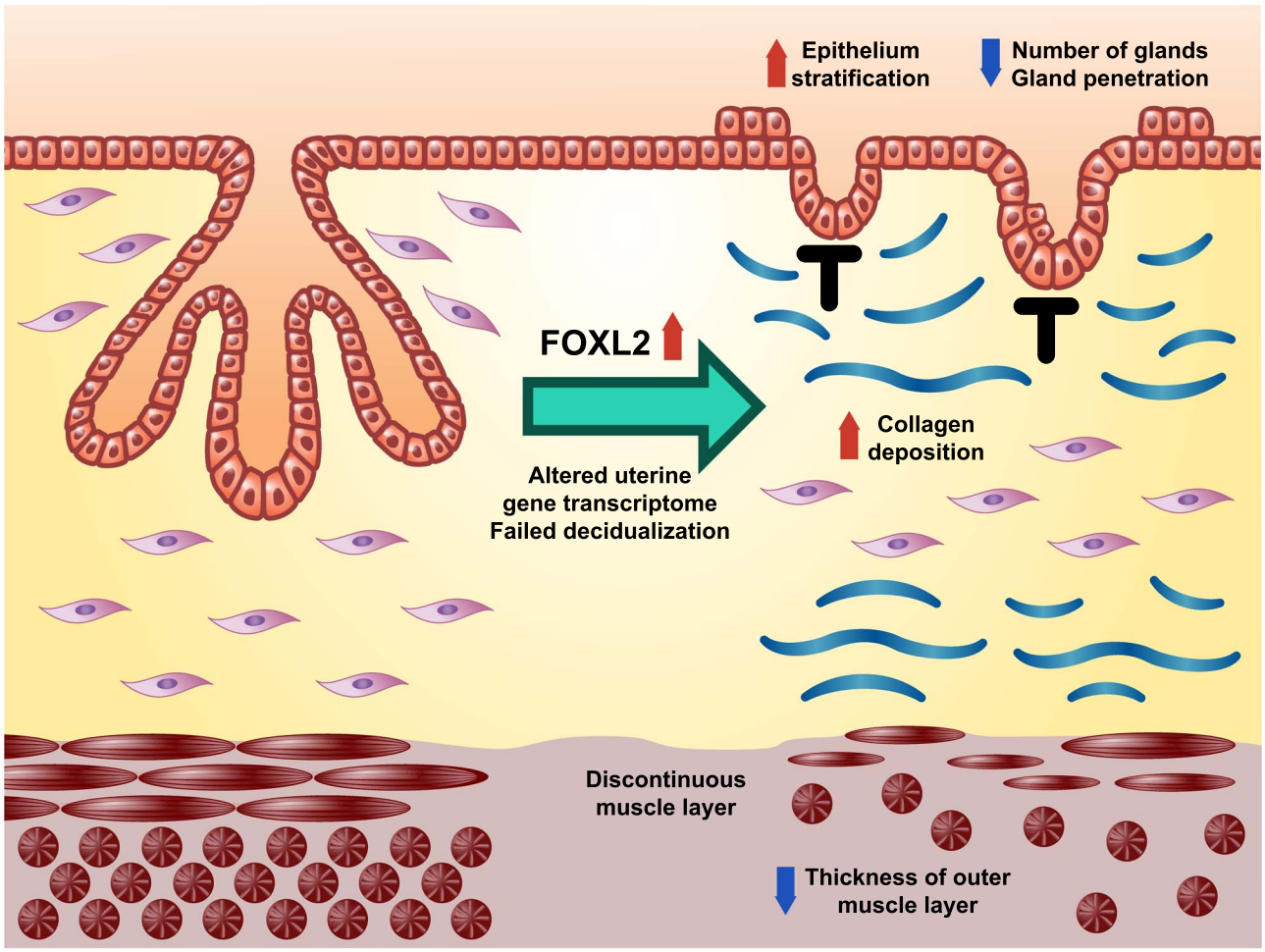

Key words: FOXL2, adenogenesis, myometrial, fibrosis, stratification.

Introduction

Forkhead Box L2 (FOXL2) is a transcription factor that contains a forkhead domain and a polyalanine tract. In addition to the human endometrium, FOXL2 is also expressed in the ovaries, the pituitary, including the gonadotrophs and some thyrotropes [1, 2, 3]. Germline mutation in FOXL2 has been associated with the blepharophimosis-ptosis-epicanthus inversus syndrome, characterized by eyelid malformation with or without primary ovarian insufficiency in humans [4]. Similarly, *Foxl2*$^{-/-}$ mice display premature ovarian failure [5, 6]. The ablation of *Foxl2* at different stages of ovarian development demonstrated that *Foxl2* is a major regulator for sex differentiation and maintenance of the ovary from the embryonic stage to adulthood [7–9]. In the pituitary, gonadotroph specific deletion of *Foxl2* in mice led to subfertility in both females and males due to Follicle-stimulating hormone (FSH) deficiency [10]. Both in vitro and in vivo models suggest that FOXL2-SMADs complexes can bind at the *Follicle Stimulating Hormone Subunit Beta* promoter to regulate its transcription [11–15]. FOXL2 also plays an important role in cancer development. It can suppress proliferation and promote apoptosis [16, 17]. Its mutation is present in most adult-type granulosa-cell tumors and cervical cancers [16, 18, 19]. Taken together, FOXL2 is pivotal for the regulation of reproductive development and the hypophyseal-ovarian axis.

There are limited studies about FOXL2 functions in the uterus. FOXL2 is detected in the stroma and glandular epithelium of cow uterus throughout the estrous cycle with much higher levels during luteolysis, as progesterone treatment decreases its expression [20]. FOXL2 is also detected in the stroma and myometrium of mouse uterus, and conditional deletion of *Foxl2* by *Pgr*^{cre} reduced the stroma compartment while altering myometrial thickness and disrupting myometrial morphology [21]. In contrast, a recent study reported that FOXL2 is mainly detected in the epithelium and myometrium, but not stroma in the mice [22]. In women with endometriosis, the eutopic endometrium and ectopic extrauterine tissues display altered gene expression signatures, including higher expression levels of FOXL2 [3]. In order to investigate the role of FOXL2 in embryo implantation, FOXL2 expression has been attenuated or enhanced in human endometrial cancer cell lines resulting in disruption of embryo attachment in vitro [22]. Despite

the contradictory expression patterns of FOXL2 in the uterus, these studies suggest that FOXL2 might play a crucial role in endometrial homeostasis and function.

The goal of this work is to investigate the consequences of increased FOXL2 expression in the reproductive tract by employing the mouse model of uterine FOXL2 overexpression, *Pgr*^{cre}*Foxl2*$^{LsL/+}$ (FOXL2^{OE}) and *Ltf*^{icre}*Foxl2*$^{LsL/+}$ (eFOXL2^{OE}) mice. FOXL2^{OE} mice displayed multiple changes in uterine morphology, including impaired adenogenesis, altered uterine epithelial differentiation, increased collagen deposition, and altered myometrial integrity, whereas eFOXL2^{OE} mouse uteri only showed epithelial stratification. The transcriptome of 3-month-old FOXL2^{OE} uteri identified multiple signaling altered. FOXL2^{OE} mice were infertile with defective ovaries. The disrupted uterine functions were indicated by the abolishment of decidual responses upon artificial decidualization.

Material and methods

Mice

The *Rosa26-CAG-LSL-Foxl2* mice with FOXL2 overexpression (named as *Foxl2*$^{LsL/+}$ in this paper), and *Pgr*^{cre} mice were described previously [9, 23]. *Ltf*^{icre} mice were kindly provided by Dr Sudhansu K. Dey [24]. *Foxl2*$^{LsL/+}$ mice were crossed with *Pgr*^{cre} mice to generate *Pgr*^{cre}*Foxl2*$^{LsL/+}$ mice, FOXL2 overexpression in the female reproductive tract (FOXL2^{OE}). To generate uterine epithelial FOXL2 overexpression mice, eFOXL2^{OE}, *Foxl2*$^{LsL/+}$ mice were crossed with *Ltf*^{icre} mice. All the mice were maintained on 129Sv and C57BL/6 J backgrounds. All animal studies were conducted in accordance with the *Guide for the Care and Use of Laboratory Animals* published by the National Institutes of Health and animal study protocols approved by the Institutional Animal Care and Use Committee at the National Institute of Environmental Health and Sciences.

Breeding trial

A total of 8-week-old *Pgr*^{cre} control mice and FOXL2^{OE} mice ($N = 6$ for each genotype) were mated with stud males for 6 months. The copulation plug and delivery date for the first generation were recorded, and the pups delivered and survival rate were checked daily.

Tissue collection

Postnatal day (PND) 21, 3-month-old, 8-month-old Pgr^{cre}, and FOXL2^{OE} mouse ovaries and uteri were collected at diestrus stage ($N = 6$). The samples were fixed in 4% PFA, dehydrated, cleared, and embedded in paraffin for histology and immunohistochemistry. Blood was collected from 3-month-old diestrus *Pgr*^{cre} and FOXL2^{OE} mice for serum hormone analysis. A total of 3-month-old *Pgr*^{cre} ($N = 3$) and FOXL2^{OE} ($N = 4$) diestrus uterus were used for RNA-seq ($N = 3$–4). A total of 3-month-old *Ltf*^{icre} and eFOXL2^{OE} females were mated with stud males. The morning the plug was detected was defined as pregnancy day 0.5. The *Ltf*^{icre} and eFOXL2^{OE} mice ($N = 6$) were sacrificed at pregnancy day 3.5; the uteri were collected and embedded in paraffin.

Superovulation

PND21 *Pgr*^{cre} and FOXL2^{OE} mice were injected with 3.25 IU of equine chorionic gonadotropin. A total of 48 h later, the mice were injected with 2 IU human chorionic gonadotropin. After 16 h, the mice were sacrificed. Blood was collected for serum hormone analysis. Oviducts were flushed for oocyte counting. The ovaries were fixed for paraffin embedding, $N = 6$.

Serum hormone analysis

Blood was collected by retro-orbital bleeding. After clotting at room temperature (RT) for 1 h, the blood samples were centrifuged at 2000 g at RT for 10 min. Serum was collected into a new tube and stored at −80°C. The serum samples were shipped to The Center for Research in Reproduction Ligand Assay and Analysis Core, University of Virginia for luteinizing hormone, FSH, estradiol, and progesterone analysis, $N = 6$.

Artificial decidualization

Pgr ^{cre} and FOXL2^{OE} mice were ovariectomized at 6 weeks old. After 2 weeks, the mice were subcutaneously (s.c.) injected with 100 ng 17β-estradiol (E8875, Sigma) each day for 3 consecutive days, rested for 2 days, then given daily s.c. the injections of 1 mg progesterone (P0130, Sigma) and 6.7 ng 17β-estradiol for 3 days. On the third day, 50 ul corn oil was injected into one uterine horn 6 h after the hormone injections. The mice were maintained with daily s.c. the injections of 1 mg progesterone and 6.7 ng 17β-estradiol for 5 days, and the uteri were collected on the sixth day. The uterine horns of both the oil injected and uninjected sides were weighed, $N = 6$.

Histology and Masson's trichrome staining

Paraffin-embedded tissues were sectioned at 5 μm, and a subset of sections was stained with hematoxylin solution, Harris modified (Sigma-Aldrich), and eosin (Sigma-Aldrich) for histology. A subset of sections was submitted to National Institute of Environmental Health and Science (NIEHS) histology Core for Masson's trichrome staining, $N = 3$.

Immunohistochemistry and immunofluorescence

A total of 5 μm paraffin sections were dewaxed and rehydrated for immunohistochemistry. After antigen retrieval, endogenous peroxidase blocking and serum blocking, they were incubated with primary antibody at 4°C overnight, including FOXL2 (1:600, ab5096, Abcam), Histidine HIS tag (1:300, ab9108, Abcam), estrogen receptor 1(ESR1; 1:100, ACA054C, Biocare Medical), Progesterone receptor PGR (1:400, 8257, cell signaling), Forkhead Box A2 FOXA2 (1:400, 8186, cell signaling), Tumor protein P63 P63 (1:800, 39692 cell signaling), and KI67 (1:1000 ab15580, Abcam).

For immunohistochemistry, on the second day, the slides were incubated with 1:500 biotin-conjugated ant-rabbit (BA-1000, Vector Laboratories), antigoat (BA-9500, Vector Laboratories) secondary antibody for 1 h at RT, respectively, followed by the ABC reagent (PK-6100, Vector Laboratories) for 1 h at RT. Signal was developed by DAB (3, 3 -diaminobenzidine) (SK-4105, Vector Laboratories) for 30s. The slides were counterstained with hematoxylin, dehydrated, cleared, and mounted by Permount medium (Thermo Fisher, Waltham, MA, USA). The images were taken using an Axiocam microscope camera (Zeiss), $N = 3$.

For immunofluorescence, on the second day, the slides were incubated with Alexa Fluor® 647 goat antirabbit secondary antibody (1:300, ab150079, Abcam) for 1 h at RT. The slides were mounted by ECTASHIELD® Antifade Mounting Medium with DAPI (H1200, Vector Laboratories). The images were taken under Zeiss 710 confocal microscopy.

Quantification of the number of glands, gland penetration, thickness of circular muscle layer, and Immunohistochemistry staining of KI67, PGR, and ESR1

The number of glands was calculated in the cross-section of the mouse uterus. For each mouse, three different cross sections were used, and the average number of three sections was presented. The gland penetration was defined as the closest distance between the gland and the uterine lumen. Similar to the gland number, the gland penetration is calculated in three different sections of each mouse. The gland penetration of each gland was presented. A total of six mice were calculated in each group.

The thickness of the inner (circular) and outer (longitudinal) muscle layer, defined as the closest distance from the outside to the inside border, was counted at four random locations of a cross-section of the uteri. The average of four locations was presented. A total of three mice were calculated in each group.

The immunohistochemistry staining of Ki67, PGR, and ESR1 was counted by the H-score method [25]. Specifically, the staining in all the sections were divided into three stages based on its intensity. Stage 0: no staining; Stage 1: weak; Stage 2: medium; Stage 3: strong.

$$\text{H-score} = (\text{stage 1 cell } \%) \times 1 + (\text{stage 2 cell}\%) \times 2 + (\text{stage 3 cell}\%) \times 3$$

One uterine cross-section from one mouse was counted. A total of three mice were calculated in each group.

RNA-seq analysis

Total RNA was isolated from 3-month-old Pgr^{cre} and FOXL2^{OE} diestrus uteri using RNeasy mini kit (Qiagen). The library was prepared using TruSeq RNA Library Prep kit (Illumina) and subsequently sequenced using Nextseq 500. The sequencing reads with quality score < 20 were filtered using a custom perl script. The adaptor sequence was removed using Cutadapt (v1.12). The reads were aligned to mm10 genome using STAR aligner (v2.5.2b) and counted using featureCounts (v1.5.0-p1) function in Subread program. The differential expressed genes (DEG) between Pgr^{cre} and FOXL2^{OE} were identified using R package "DESeq2." The threshold was set as "maximal FPKM $\geq$ 1, unadjusted $P < 0.05$, fold change $\geq$ 1.5 (up-regulated) or ≤ -1.5 (down-regulated)." The RNAseq data are deposited in NCBI Gene Expression Omnibus repository (GEO accession number) GSE140047.

The functions of the DEG were analyzed by Ingenuity Pathway Analysis (IPA, Qiagen) and DAVID Functional Annotation Bioinformatics Microarray Analysis [26, 27].

Statistical analysis

The normality of the data was tested by the Kolmogorov–Smirnov test. The equal variance of the data was tested by Levene's test. The total number of pups, the number of ovulated oocytes, the serum levels of progesterone, 17β-estradiol, FSH and luteinizing hormone (LH), the number of uterine glands, the uterine gland penetration, the thickness of muscle layer, and the H-score of Ki67, ESR1, and PGR immunohistochemistry staining were compared by two-tail, Student's t-test. The significance was set at $P < 0.05$.

Results

Foxl2 transgene expression in the mouse uterus

Increased Foxl2 expression was achieved by crossing mice with a conditionally active transgene, $Foxl2^{LsL/+}$ [9] with the Pgr^{cre} allele [23] generating the $Pgr^{cre/+}Foxl2^{LsL/+}$ (FOXL2^{OE}) mouse. Immunohistochemical analysis was used to detect the expression of endogenous FOXL2 and the *Foxl2* transgene in the mouse uterus. In wild type mice, FOXL2 expression was observed in the endometrial stroma and blood vessels, and to a lesser extend in the epithelial and myometrial compartment of the uterus (Supplementary Figure S1A–C) as previously reported [21]. The analysis of the uterine expression of the *Foxl2* transgene in the FOXL2^{OE} showed an increased expression in a subset of uterine luminal and glandular epithelium, and sporadic staining in the myometrium (Supplementary Figure S1D–F). Due to the fact that FOXL2 is already highly expressed in the endometrial stroma cells of the Pgr^{cre} mice, it is difficult to distinguish the endogenous FOXL2 from the expression of the *Foxl2* transgene. Since the HIS-tag epitope was incorporated into the *Foxl2* transgene, the expression of the transgene in the endometrial stroma was determined by immunofluorescence staining for His-tag [9]. Compared with the Pgr^{cre} mouse uterus (Supplementary Figure S1G–I), His-tag displayed strong nuclear staining of the FOXL2 transgene in all compartments of the uterus (Supplementary Figure S1J–L). This analysis demonstrated that the *Foxl2* transgene was expressed in not only the epithelial and myometrial compartment, but also the stroma.

Abnormal uterine morphology by uterine FOXL2 overexpression

Macroscopic examination of the uterus showed that at PND21 the uterine size of the Pgr^{cre} and FOXL2^{OE} were comparable (Figure 1A and D). However, the uteri of FOXL2^{OE} mice were thinner compared with the control mice at 3 and 8 months at diestrus stage (Figure 1B, C, E, and F). Histological analysis identified alterations in all compartments of the uterus. Analysis of the uterine epithelium showed altered uterine epithelial cell differentiation. p63 is a marker for epithelial stratification [25]. Although the control Pgr^{cre} mice showed a uterine epithelium lined with a single layer of columnar cells (Figure 1G–I), the FOXL2^{OE} showed the presence of basal cells with P63 positive staining in glandular and luminal epithelium (Figure 1J–O). In addition to the altered uterine epithelial differentiation, there was altered uterine gland morphology indicating a defect in adenogenesis.

Adenogenesis in rodents is a hormone-independent process before puberty, but is maintained by estrogen after puberty [28]. In the FOXL2^{OE} uterus, pre-pubertal gland development was already impaired at PND21, demonstrated by a decrease of the gland number and by the decreased penetration of the glands into the stroma (Figure 2A, D, G, J, and K). The defect in adenogenesis became more pronounced during the post-pubertal period. The Pgr^{cre} mice showed a remarkable increase in both the number of glands and gland penetration into the stroma compared with PND21. In contrast, the uterine glands of the FOXL2^{OE} remained at a lower number and few of them were able to penetrate the stroma. The impaired adenogenesis may result from a defect in gland growth or from the uterine stroma not providing the appropriate milieu for gland development (Figure 2B, C, E, F, and H–K).

In order to determine the impact on FOXL2 expression on the endometrial stroma biology, the composition of the stromal extracellular matrix of the mouse uterus, Pgr^{cre}, and FOXL2^{OE} mouse uteri was examined by Masson's trichrome staining. Blue staining indicating collage deposition was increased with age in both Pgr^{cre} and FOXL2^{OE} mice (Figure 3A–F). But at each age, the blue staining was much stronger in FOXL2^{OE} uterus suggesting increased collagen

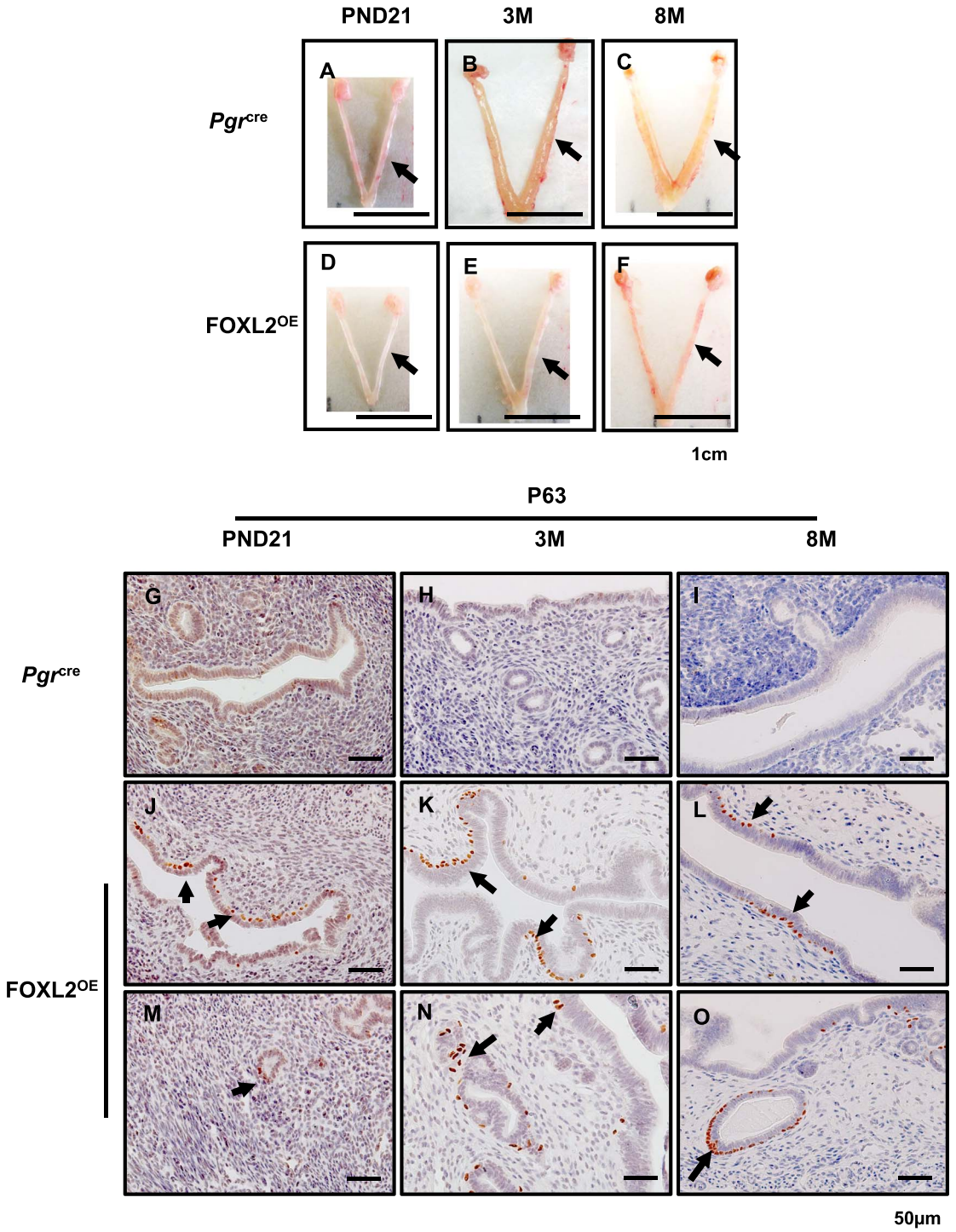

Figure 1. FOXL2^{OE} mice displayed thin uterus and stratified uterine epithelium. The representative uterine images of *Pgr*^{cre} (A–C) and FOXL2^{OE} mice (D–F) at PND21 (A and D), 3 M (B and E), and 8 M (C and F). The uteri were much thinner in FOXL2^{OE} mice compared with *Pgr*^{cre} mice at 3 M and 6 M. Basal cell marker, P63, staining in the uterus of *Pgr*^{cre} (G–I) and FOXL2^{OE} mice (J–O) at PND21 (G, J, and M), 3 M (H, K, and N), and 6 M (I, L, and O). P63 positive basal cells in the uterus indicate epithelium stratification. They were found at the basal side of some luminal epithelium (J–L) and some glandular cells (M–O) in the FOXL2^{oe} uterus. PND: postnatal day; M: months old. Arrow indicates stratified epithelium. $N = 3$ for each genotype and age group. Arrow in A–F refers one uterine horn. Arrow in J–O indicates stratified epithelium.

deposition (Figure 3 A–F). The changes in the composition of the extracellular matrix may impede the ability of the glands to fully develop.

In addition to the impact of *Foxl2* transgene expression on the uterine endometrium, the transgene also affected the morphology of the myometrium. Immunohistochemistry was conducted to assay the expression of alpha-smooth muscle actin (α-SMA), one of the common markers of mature myometrium [4]. The α-SMA positive myometrial cells were identified in both *Pgr*^{cre} and FOXL2^{OE} mouse uterus with no obvious changes of its staining intensity

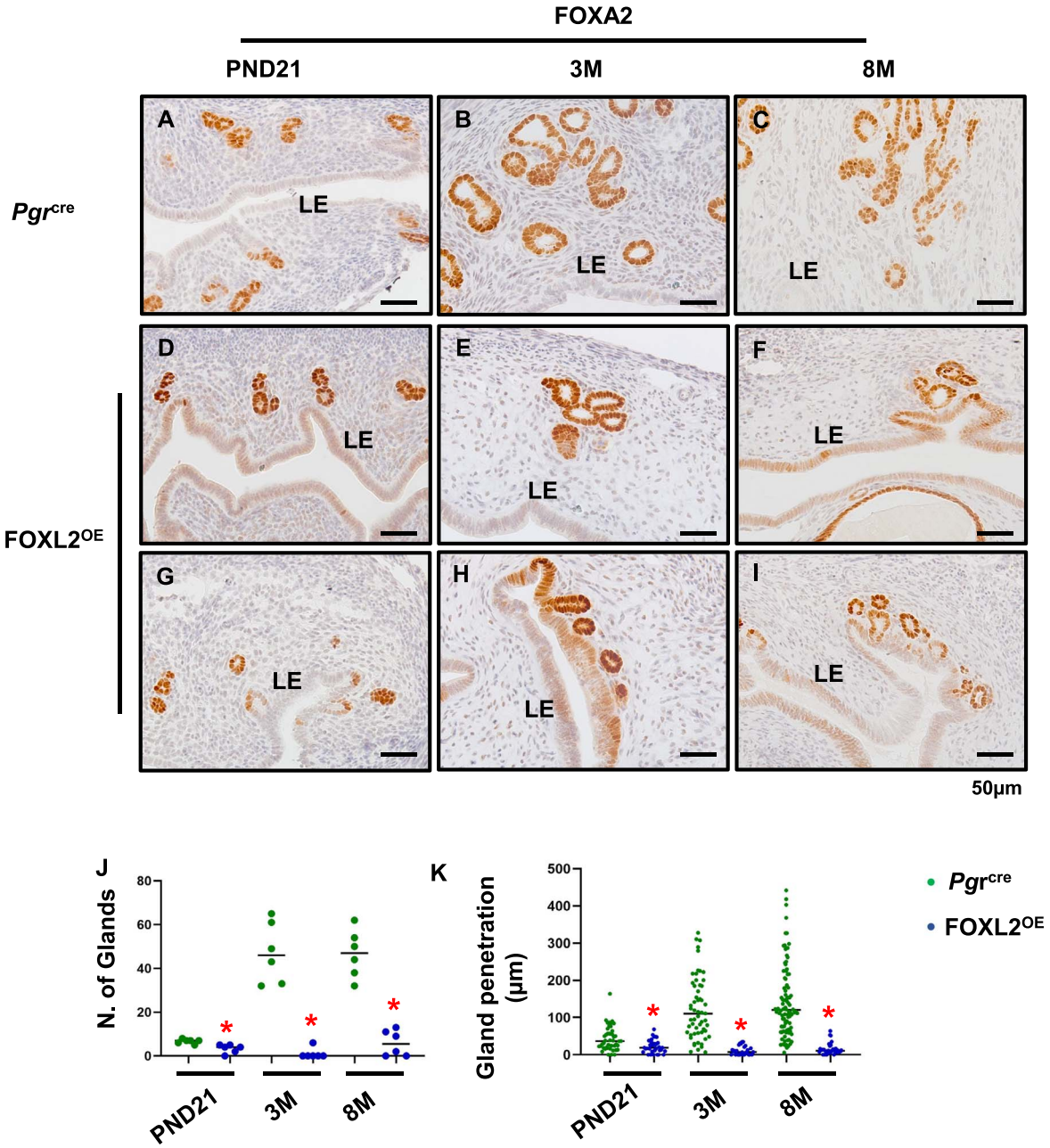

Figure 2. Disrupted adenogenesis in FOXL2^{OE} mice. FOXA2 labeled glands in *Pgr*^{cre} (A–C) and FOXL2^{OE} (D–I) uterus at PND21 (A, D, and G), 3 M (B, E, and H), and 8 M (C, F, and I). The number of glands was calculated in two cross sections per mouse, in total six mice (J). The penetration of glands was defined as the closest distance of the glands to the adjacent luminal epithelium and calculated in one longitudinal section per mouse, in total six mice (K). PND: postnatal day; M: months old. $*P < 0.05$. FOXL2^{OE} compared with *Pgr*^{cre} mice at the same age.

(Figure 3 G–O). However, although the myometrium of *Pgr*^{cre} mouse uteri showed the inner layer of myometrium to be a continuous layer of circular smoother muscle surrounding the endometrium (Figure 3G–I), the inner smooth muscle layer of the FOXL2^{OE} mouse myometrium was discontinued at several loci (Figure 3J–O, arrows). This abnormality was detected in the FOXL2^{OE} not the *Pgr*^{cre} uterus as early as PND21 (Figure 3G, J, and M), and remained at 3 months (Figure 3H, K, and N) and 8 months (Figure 3I, L and O). The thickness of the outer longitudinal smooth muscle layer showed an increasing trend with age in *Pgr*^{cre} but not FOXL2^{OE} mice from PND21 to 8 months (Figure 3G–P). Statistically, the thickness of the outer muscle layer was decreased in the FOXL2^{OE} mice at 3 and 8 months old (Figure 3G–P).

Altered uterine epithelial differentiation but not adenogenesis, stromal fibrosis, or myometrial structures by epithelial FOXL2 overexpression

The FOXL2^{OE} mouse uterus exhibited FOXL2 overexpression in all the uterine compartments. In order to investigate the impact of altered FOXL2 functions specifically in the uterine epithelium, we bred the FOXL2^{LSL} mice with the uterine epithelial *Ltf*^{icre} to generate

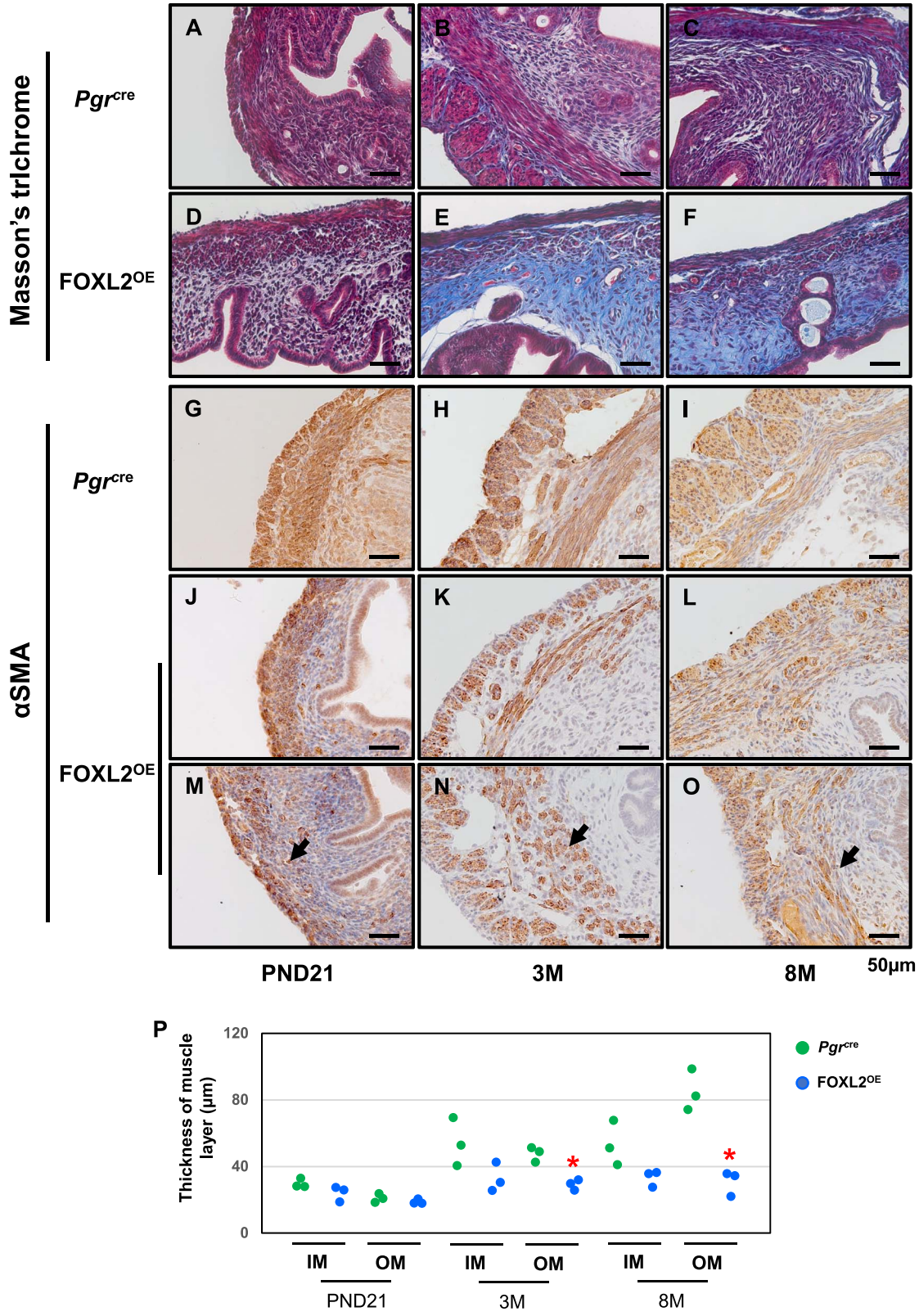

Figure 3. Stroma fibrosis and defective myometrium in FOXL2^{OE} mice. Masson's trichrome staining in *Pgr*^{cre} (A–C) and FOXL2^{oe} (D–F) uterus at PND21 (A and D), 3 M (B and E), 8 M (C and F). Increased blue staining in the stroma of FOXL2^{OE} uterus suggested increased collagen deposition. αSMA staining in *Pgr*^{cre} (G–I) and FOXL2^{OE} (J–O) uterus at PND21 (G, J, and M), 3 M (H, K, and N), 8 M (I, L, and O). The thickness of the inner (circular) and outer (longitudinal) muscle layer was calculated in one cross-section of each mouse (P). The thickness of outer layer was decreased at 3 M and 8 M and the inner muscle layer was discontinued in the FOXL2^{OE} uterus. PND: postnatal day; M: months old; IM: Inner muscle layer; OM: Outer muscle layer. The arrow indicates the discontinued muscle layer. $N = 3$ for each genotype and age group. $*P < 0.05$, FOXL2^{OE} compared with *Pgr*^{cre} mice at the same age.

epithelial overexpressing FOXL2, eFOXL2^{OE} mice. *Ltf*^{ice} expresses Cre recombinase specifically in the uterine epithelium [24], FOXL2 and His-tag staining confirmed that the FOXL2 overexpression is limited in a subset of luminal and glandular epithelium of eFOXL2^{OE} uteri (Supplementary Figure S2).

Uterine morphology was assayed at D3.5 of pregnancy. The gross uterine morphology was similar between *Ltf*^{icre} and eFOXL2^{OE} females (Figure 4A and B). The thread-like uterus observed in FOXL2^{OE} mice (Figure 1D–F) was not found in eFOXL2^{OE} mice. Histological analysis of the uterus of the eFOXL2^{OE} mice showed epithelial stratification with the presence of P63 positive basal cells (Figure 4C and D), which was also observed in the FOXL2^{OE} mouse uterus (Figure 4G–O). Unlike the FOXL2^{OE}, eFOXL2^{OE} mouse uteri did not show any alteration in the number of uterine glands, as determined by FOXA2 staining (Figure 4E and F), or in the uterine stromal fibrosis, as determined by Masson's trichrome (Figure 4G and H), or in their myometrium morphology, as determined by αSMA staining (Figure 4I and J). These suggested that epithelial overexpression of FOXL2 impacted uterine epithelial stratification. However, uterine gland development, stromal fibrosis, and myometrial morphology were mainly affected by the extra epithelial overexpression of FOXL2. Based on this, the FOXL2^{OE} mice were used for further studies of the impact of FOXL2 overexpression in uterine transcriptome and functions.

Foxl2 transgene impact on the uterine transcriptome

In order to determine the impact of the *Foxl2* transgene expression on the mouse uterus at the molecular level, RNA-Seq was conducted on the uteri of 3-month-old *Pgr*^{Cre} and FOXL2^{OE} mice. Since uterine transcriptome largely depends on hormone regulation, we collected all the uteri at diestrus stage. In total, 3515 genes were differentially expressed in the FOXL2^{OE} compared with the *Pgr*^{cre} uterus (1746 upregulated and 1769 downregulated genes, respectively, Figure 5A, the detailed gene list is in the supplemental excel file). Ingenuity pathway analysis identified multiple signaling pathways altered in the FOXL2^{OE} uterus (Figure 5B, the full list of the altered pathways is in the supplemental excel file). The altered pathways included pathways regulating cell proliferation (cyclins and cell cycle regulation and estrogen-mediated S-phase entry, enhanced role of Serine/threonine Kinases (CHK) proteins in cell cycle checkpoint control), extracellular matrix production (inhibition of matrix metalloproteases, suppressed collagen receptor, Glycoprotein VI (GP6) signaling, and Hepatic Fibrosis/Hepatic Stellate activation), and Wnt/β-catenin signaling. These pathways likely contribute to the altered epithelial and stroma phenotype observed in the FOXL2^{OE} mouse uterus. Here, we would like to mention that several collagen genes in the GP6 signaling pathways were decreased in FOXL2^{OE} uterus, such as *Col1a1* and *Col6a1*, which is in contrast to the increased collagen deposition. However, the collagen degradation genes in the inhibition of matrix metalloproteases were also suppressed in FOXL2^{OE} uterus, such as MMP2, MMP15 suggesting that the inhibition of the matrix degradation might be the major reason for the increased collagen deposition in the FOXL2^{OE} uterine.

The RNA-Seq results identified several critical genes that are known to have an important role in the uterine phenotypes. We next validated the protein expression of selected genes by immunohistochemistry and performed semi-quantification using the H-score method. Since genes involved in cell cycle regulation were altered, *Ki67* expression was assayed. *Ki67* expression was decreased in our RNA-Seq results (Fold change (FC) = −5.86, $P < 0.001$), and immunohistochemistry confirmed the decreased protein levels of KI67 in the luminal epithelial of the FOXL2^{OE} uterus (Figure 6A–D, M, and P, open arrow). *Esr1* and *Pgr* are the major receptors for ovarian hormones and regulators of uterine function [33]. Our RNA-Seq results showed mRNA levels of *Esr1* (FC = 1.51, $P < 0.001$) were increased and *Pgr* (FC = -1.26, $P = 0.035$) was decreased in the FOXL2^{OE} uterus. Immunohistochemistry showed much higher protein levels of ESR1 in the uterine luminal epithelium (Figure 6E–H, N, and Q, solid arrow) and much lower protein levels of PGR in the uterine luminal epithelium and stroma (Figure 6I–L, O, and R, open arrow) of the FOXL2^{OE} mice.

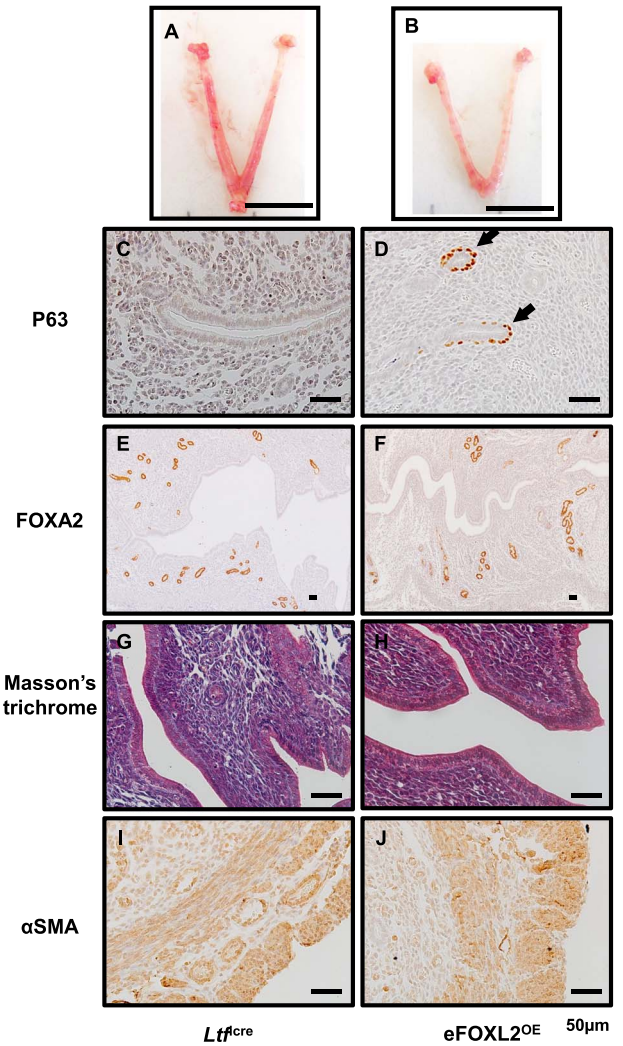

Figure 4. eFOXL2^{OE} exhibited epithelium stratification but no adenogenesis, stroma fibrosis, and myometrial defects. The representative uterine images of *Ltf*^{icre} (A) and eFOXL2^{OE} mice (B) at Pregnancy D3.5. P63 (C and D), FOXA2 (E and F), Masson's trichrome (G and H), and αSMA (I and J) staining in *Ltf*^{icre} (C, E, G, and I) and eFOXL2^{OE} (D, E, H, and J) uterus. Basal cells with P63 positive staining was detected in the luminal and glandular epithelium of eFOXL2^{OE} uterus. No changes were observed in FOXA2 labeled uterine glands, Masson's trichrome staining, and αSMA labeled muscle layers. Arrow indicates stratified epithelium. $N = 3$.

Infertility in FOXL2^{OE} mice

As we already observed multiple uterine functions in the FOXL2^{OE} mice, we decided to investigate the impact of the *Foxl2* transgene

A

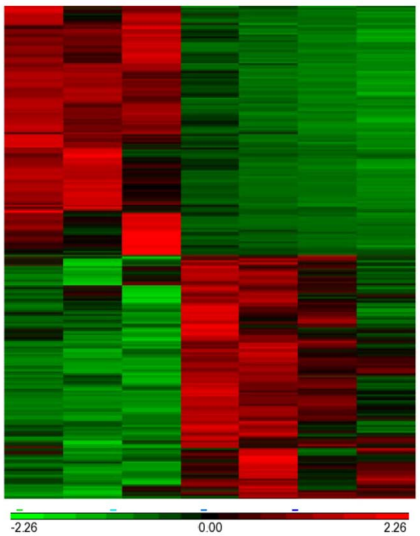

B

Ingenuity Canonical Pathways	-log(p-value)	z-score	Molecules
Cyclins and Cell Cycle Regulation	4.39	-3.128	CDKN2A,SUV39H1,CDK4,CCNB2,CDKN2C,E2F3,CDKN2B,CCNA2,TGFB1,PPM1J,PPP2R2C,E2F2,E2F8,CDC25A,HDAC9,CCNE2,TFDP1,WEE1,CDK1,CCNB1,SKP2,CCNE1,CCND2,E2F1,E2F7,PPP2R2B
Estrogen-mediated S-phase Entry	7.39	-2.84	CCNE2,TFDP1,CDK4,E2F3,RBL1,CDK1,SKP2,MYC,CCNA2,CCNE1,E2F1,E2F7,ESR1,E2F8,E2F2,CDC25A
Role of CHK Proteins in Cell Cycle Checkpoint Control	4.66	2.496	CDC25C,PLK1,RPA1,RFC5,E2F3,CDK1,CHEK1,PCNA,RFC4,PPM1J,PPP2R2B,E2F1,E2F7,RFC2,SLC19A1,CLSPN,PPP2R2C,BRCA1,E2F2,E2F8,CDC25A
Inhibition of Matrix Metalloproteases	2.64	1.387	TIMP3,MMP28,MMP3,MMP15,MMP2,TFPI2,ADAM12,TIMP1,THBS2,MMP11,A2M,MMP9,MMP19
GP6 Signaling Pathway	5.5	-3.162	ITGA2B,COL4A5,PIK3R1,PIK3R5,COL9A3,COL4A2,Col17a1,COL6A6,COL26A1,COL28A1,PRKCZ,Col6a4,ITGB3,COL16A1,COL5A1,LAMC1,FGFR3,COL6A1,LAMB1,COL22A1,COL18A1,PIK3C2B,COL5A2,COL4A1,PRKCQ,COL6A2,APBB1IP,FGFR1,COL12A1,LAMA2,LAMC3,COL20A1,COL1A1,COL23A1,SYK,PIK3R6,COL11A1,COL9A2,COL7A1,PRKCB
Wnt/β-catenin Signaling	1.13	-2.414	CDKN2A,FZD10,TCF4,SFRP2,FRZB,TGFBR3,SOX12,WNT6,ACVR2B,FZD1,BCL9,SOX13,HNF1A,MYC,TGFB1,PPM1J,PPP2R2C,FZD2,SOX5,SOX7,AXIN2,APPL2,WNT9A,DKKL1,ACVR1B,UBD,CDH5,PPP2R2B,CD44,NR5A2,LEF1,TCF7L2
Hepatic Fibrosis / Hepatic Stellate Cell Activation	10.7	#NUM!	CTGF,COL9A3,MYL6B,COL28A1,Col6a4,VEGFA,TGFB1,SERPINE1,MYL3,PDGFRB,TNFRSF11B,IL4R,COL4A1,FGFR1,MYH14,VEGFC,MMP2,MYL9,IGF2,COL23A1,COL7A1,IGFBP4,COL4A5,FN1,FGF2,LEPR,CCL5,MYH11,COL4A2,Col17a1,PDGFC,COL6A6,COL26A1,FAS,COL5A1,COL16A1,COL6A1,CCL2,IGF1,TIMP1,NGFR,HGF,IGF1R,COL22A1,LBP,COL18A1,TNFRSF1B,EGFR,COL5A2,COL6A2,FLT1,EDNRB,COL12A1,FLT4,COL20A1,BAX,COL1A1,TLR4,COL11A1,KDR,COL9A2,A2M,MMP9
Gap Junction Signaling	2.84	#NUM!	TUBA1B,DBN1,GRIA1,PIK3R1,GJB3,NOTUM,PIK3R5,PLCH2,TUBB,GRIA4,PRKCZ,TUBB2B,FGFR3,MRAS,PRKAR1B,TUBB4A,TUBA1C,Gucy2g,ACTA1,GUCY1B1,EGFR,PIK3C2B,TUBB3,ADCY2,PRKCQ,GUCY1A1,TUBB4B,FGFR1,TUBG1,GNAI1,GJA5,NOV,PRKG1,TUBA1A,TUBB6,LPAR1,NPR1,GJA3,ADCY1,SGSM3,PIK3R6,MAPK7,ADCY7,GJB1,PRKCB

Figure 5. Transcriptomic changes of *Pgr*^{cre} and FOXL2^{OE} at 3 M diestrus stage ($P < 0.05$, fold change > 1.5, < -1.5). Heating map showed cluster of differentially expressed genes in *Pgr*^{cre} and FOXL2^{OE} (A). Ingenuity pathway analysis identified top altered signaling pathways (B). $N = 3–4$.

expression by a 6-month breeding trial. Adult *Pgr*^{cre} and FOXL2^{OE} female mice were placed with male mice and allowed to breed for 6 months. During the 6 months, *Pgr*^{cre} females produced 36 ± 2.35 pups/female, whereas FOXL2^{OE} females produced no offspring (Figure 7A), This demonstrated that the FOXL2^{OE} female mice were infertile. In order to determine the cause of infertility, female mice were examined for the presence of a postcoital vaginal plug after being placed with a male mouse. No copulation plug was ever detected in FOXL2^{OE} females during the breeding trial. Since mating occurs in female mice during the estrus stage of the cycle, the ability of the FOXL2^{OE} mice to undergo a normal estrus cycle was analyzed by vaginal cytology over a 3-week period. We found FOXL2^{OE} female mice did not show the presence of a vaginal estrus cycle and were in a constant state of diestrus (Figure 7 B and C). Analysis of estrogen and progesterone levels in the FOXL2^{OE} mice reveals that they were comparable with those of *Pgr*^{cre} mice in the diestrus

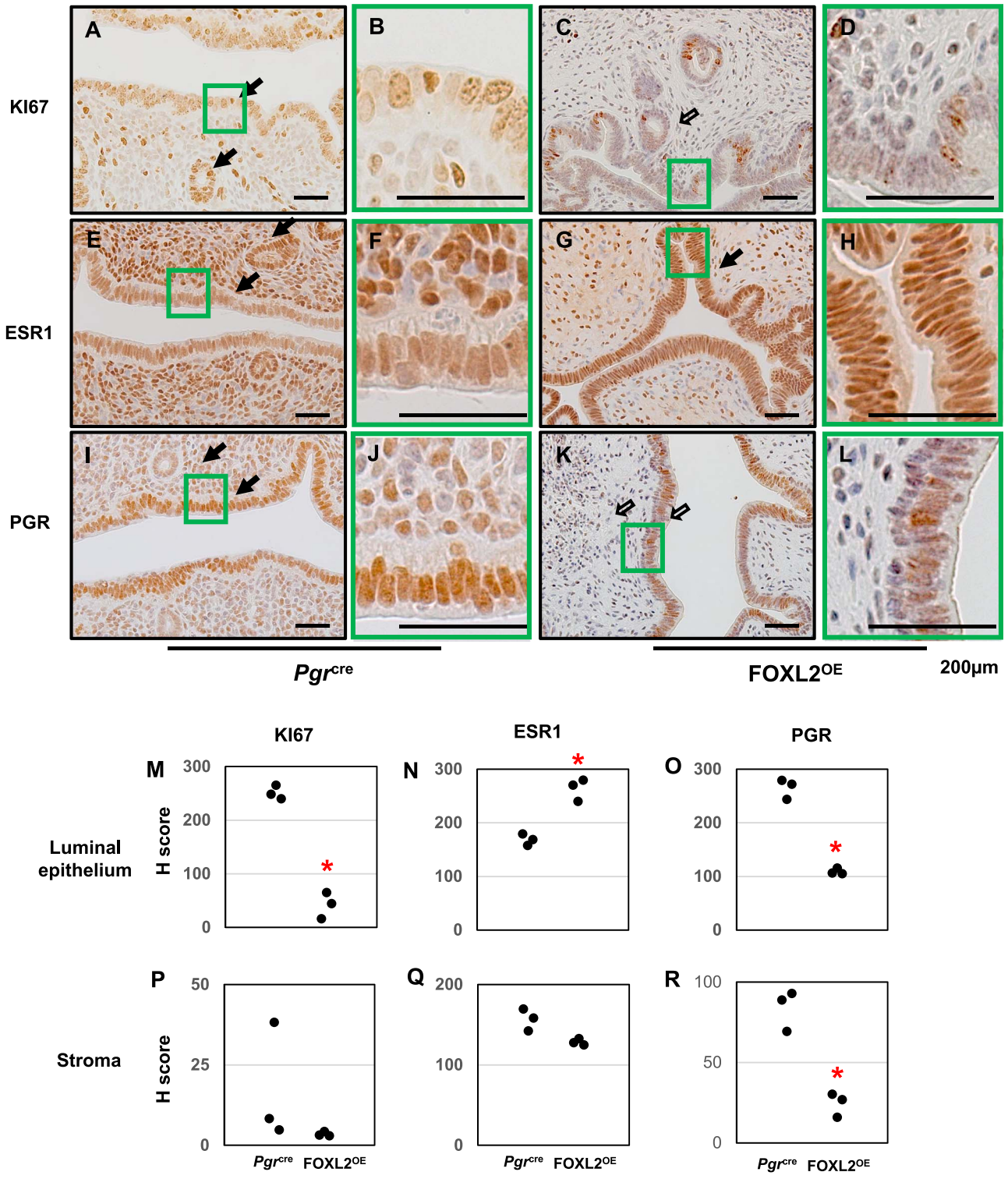

Figure 6. Protein expressions of KI67, ESR1, and PGR in FOXL2^{OE} uterus at 3 M diestrus stage. Immunohistochemistry of KI67 (A–D), ESR1 (E–H), PGR (I–L) in *Pgr*^{cre} (A, B, E, F, I, and J), and FOXL2^{OE} (C, D, G, H, K, and L) uterus. H-score of the immunohistochemistry of Ki67 (M and P), ESR1 (N and Q), and PGR (O and R) in the uterine luminal epithelium and stroma showed ESR1 was increased in the epithelium, PGR and KI67 were decreased in the epithelium of the FOXL2^{OE} uterus. Solid arrow indicates cells with strong staining. Open arrow indicates cells with weak staining. $N = 3$.

stage (Supplementary Figure S3A and B). This confirmed that the continuous diestrus stage in the FOXL2^{OE} mice not only reflected on the vagina cytology, but also by the ovarian hormone levels.

Altered ovarian function in FOXL2^{OE} mice

The estrus cycle of mice is driven by steroid hormones produced by the ovaries. Since *Pgr* is transiently expressed in the ovarian

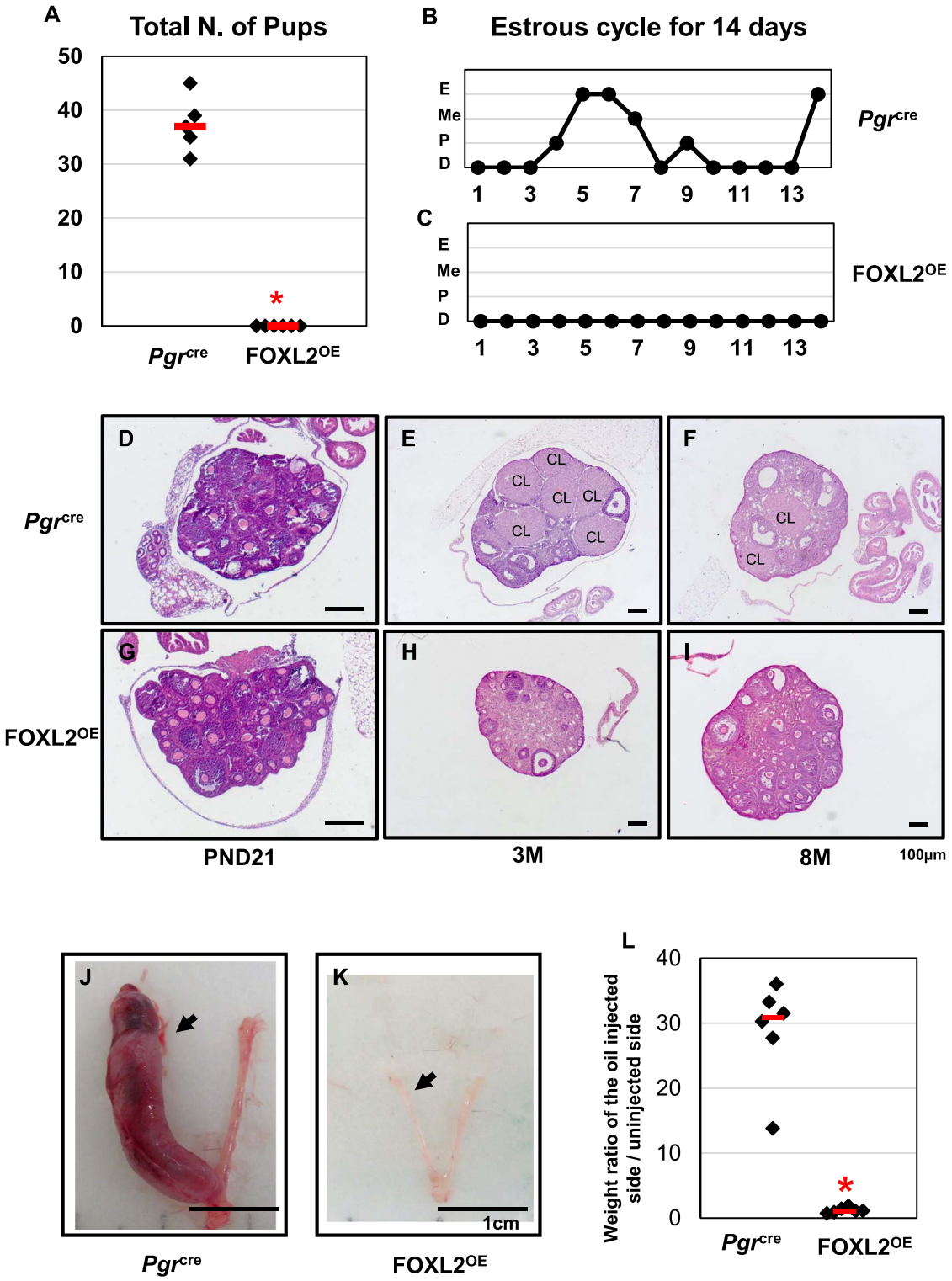

Figure 7. FOXL2^{OE} mice were infertile with abolished decidual responses. All the *Pgr*^{cre} mice but none of the FOXL2^{OE} mice delivered any pups during 6-month breeding trial (A). Representative pictures of estrous cycle showed continuous diestrus in FOXL2^{OE} mice (C) in contrast to the estrous cycle showed in *Pgr*^{cre} mice (B) during 14-day period. Representative ovarian histology pictures of *Pgr*^{cre} (D–F) and FOXL2^{OE} (G–I) virgin mice at diestrus stage at the age of PND21 (D and G), 3 M (E and H), and 8 M (F and I). FOXL2^{OE} ovaries were depleted of corpus luteum. The representative pictures of the hormone primed uterus after 5-day oil injections in the *Pgr*^{cre} (J) and FOXL2^{OE} (K) mice. The weight ratio of the oil-injected side over the un-injected side uterine horn (L) confirmed that the decidualization occurred in all the *Pgr*^{cre} but none of the FOXL2^{OE} mice. Arrow indicates the oil-injected side. D: diestrus; P: proestrus; Me: metestrus; E: estrus; PND: postnatal day; M: months old; CL: corpus luteum. The arrow indicates oil injected uterine horn. $N = 6$ for each genotype and age group.

corpus luteum [30], we examined the ovaries to determine whether the acyclicity was caused by any ovarian defects. At PND21, the ovaries contained most small and medium follicles in both *Pgr*^{cre} and FOXL2^{OE} mice (Figure 7D and G). At 3 and 8 months, the ovaries of *Pgr*^{cre} mice showed follicles at different stages and multiple corpora lutea (Figure 7E and F). However, the FOXL2^{OE} mouse ovaries showed normal follicular development until antral follicle, but complete absence of corpora lutea (Figure 7H and I).

The lack of corpora lutea in the FOXL2^{OE} could be intrinsic to the ovary or could be due to a defect in neuroendocrine regulation of the ovulatory process. In order to determine the reason for the lack of corpora lutea in the FOXL2^{OE} mice, we first investigated the expression of the *Foxl2* transgene in these mice. At 3 months, both *Pgr*^{cre} and FOXL2^{OE} ovaries from the mice in diestrus showed high levels of endogenous FOXL2 in the small and medium follicles (Supplementary Figure S4A and B). However, His-tag staining detected no strong nuclear staining in *Pgr*^{cre} and FOXL2^{OE} ovaries suggesting that there is no *Foxl2* transgene expression in FOXL2^{OE} mouse ovaries (Supplementary Figure S4C and D). Therefore, the ovarian phenotype may not be due to ovarian expression of the *Foxl2* transgene since the follicles could not develop to a stage where the *Pgr*^{cre} would activate the expression of the transgene.

We next examined if the ovarian phenotype could be rescued by administering a super ovulatory regimen of gonadotropins to the mice. We found 7 of 10 *Pgr*^{cre} and 3 of 10 FOXL2^{OE} ovulated in response to the superovulation of gonadotropins. *Pgr*^{cre} mice that ovulated produced 34.3 ± 4.5 oocytes and FOXL2^{OE} mice that ovulated produced 8.3 ± 3.8 oocytes (Supplementary Figure S4I). All mice showed corpora lutea in the ovary (Supplementary Figure S4G, H, and J), and *Foxl2* transgene expression was identified by His-tag in the peri-ovulatory follicles and the corpus luteum of the FOXL2^{OE} mice (Supplementary Figure S4F and H). This indicates that FOXL2 overexpression can impair ovulation, but not impact the ability of the follicles to luteinize once ovulation has occurred.

Since one major function of the corpus luteum is progesterone synthesis, we checked the serum progesterone levels of one litter of 21-day-old mice after superovulation to test whether these corpus lutea were functional. Both the *Pgr*^{cre} and FOXL2^{OE} mice displayed increased progesterone levels in comparison to the diestrus mice with no difference between the *Pgr*^{cre} and FOXL2^{OE} mice (Supplementary Figures S4A and S5A). This indicated that FOXL2 overexpressed corpus luteum was capable of producing progesterone.

These results indicated that for the FOXL2^{OE} ovaries, the ability to respond to gonadotropin stimulation and ovulate is impaired, but the corpus luteum formation and progesterone production can be rescued by superovulation. Therefore, we proposed that the ovarian defects may partially explain the ovulation problems, but the absence of corpus luteum and the continuous diestrus levels of serum progesterone and estrogen were more likely to result from alteration in neuroendocrine regulation.

Pituitary is the direct upstream regulator of the ovary. To evaluate the functions of the pituitary, we assayed the serum levels of two gonadotropins produced by the pituitary; FSH and LH showed no difference in serum levels (Supplementary Figure S5B and C). Although the pituitary is capable of producing FSH and LH in the FOXL2^{OE} mice, we have not ruled out that the appropriate cyclic regulation of these gonadotropins is altered. Although the levels of FSH in the FOXL2^{OE} mice were not significantly different, there was a much larger variation in levels compared with that of the control *Pgr*^{cre} mice. Further studies are required to determine the role of the *Foxl2* transgene in the pituitary, which is beyond the focus of this report.

Impaired ability of the FOXL2^{OE} uterus to undergo a decidual reaction

It is true that the ovarian defects led to the infertility of the FOXL2^{OE} mice, but considering the multiple uterine morphological changes, it is possible that the uterine functions might also be altered. Since one major function of the uterus is to accommodate the embryo implantation by decidualization, the ability of the uterus to undergo a decidual reaction was assayed. The decidualization of the uterine stroma, which involves both stroma and epithelial signaling, is critical is to support pregnancy [31]. To avoid the ovary defects, female *Pgr*^{Cre} and FOXL2^{OE} mice were ovariectomized and administered an ovarian hormonal regimen combined with trauma to one uterine horn to assess the decidual response. The control mice showed an increase in the uterine size of the traumatized horn as compared with the untraumatized horn indicative of a decidual response (Figure 7J and L). In contrast, the size of the traumatized horn of the FOXL2^{OE} mice did not increase indicating the complete absence of a decidual response (Figure 7K and L). This demonstrates that altered FOXL2 expression impairs the hormonal differentiation of the uterus necessary to support pregnancy.

Discussion

In this study, we found that FOXL2 overexpression in PGR expressing cells severely impaired both the ovarian and uterine structures and functions. Since we observed constant diestrus in FOXL2^{OE} mice in which stage estrogens and progesterone are at relatively low levels, it is natural to assume that these low levels of ovarian hormones might explain some of the FOXL2^{OE} uterine phenotypes. However, the uterus of the FOXL2^{OE} mouse does not phenocopy what is observed in the ovariectomized mouse models. First, ovariectomy has never been positively correlated with epithelium stratification; instead, estrogen is required for vagina epithelium stratification [32]. The stratification was also observed in the mice with epithelial-specific overexpression of FOXL2 indicating a phenotype of uterine origin. Second, neither ovariectomy nor the ablation of PGR and ESR1 impairs prepubertal adenogenesis as observed in the FOXL2^{OE} mouse [33–35]. Since ovariectomy does impair post-pubertal glandular development, the alteration in ovarian hormone production may be partly responsible for the reduction of adenogenesis at 3 and 8 months. Third, ovariectomy has been reported to decrease collagen deposition in the uterus [36]. Finally, the reduced ovarian hormone might account for the hypotrophic myometrium, but not the discontinued smooth muscle layer [37]. According to these evidences, we conclude that the FOXL2^{OE} uterine defects are of uterine origin.

The stratified squamous uterine epithelium being observed in both FOXL2^{OE} and eFOXL2^{OE} uteri suggests that epithelial *Foxl2* transgene expression is sufficient to induce the epithelial differentiation phenotypes. Previous studies reported that multiple mouse models with enhanced estrogen signaling might stimulate the uterine stratification [38–41]. Considering the low estradiol scenario in these FOXL2^{OE} mice that are at continuous diestrus stage, alternative pathways might be involved. In our studies, we found that the Wnt/β-catenin pathway was suppressed in the 3-month-old FOXL2^{OE} mouse uterus. Wnt/β-catenin signaling interacts with

multiple estrogen signaling [42, 43]. Mice with either $Pgr^{cre/+}$ induced deletion of β-catenin in $Pgr^{cre/+}Ctnnb1^{dd}$ mice [44], or with global knockout of *Wnt7a* [45] exhibit epithelium stratification in the uterus. It is possible that FOXL2 can promote epithelial stratification by suppressing the Wnt/β-catenin pathway. The FOXL2 negative regulation on Wnt/β-catenin has also been reported in other studies. $Pgr^{cre/+}$ induced deletion of FOXL2 upregulates *Wnt4* and *Wnt7a* in the mouse uterus at PND25 [21]. FOXL2 and β-catenin have shown opposite functions on cell proliferation in ovarian cells [46].

Normal gland development in the eFOXL2^{OE} uterus suggests that epithelial FOXL2 overexpression does not impair adenogenesis. For the pre-pubertal adenogenesis, it is possible that stroma FOXL2 exert its effects through Wnt/β-catenin signaling, which has been identified to be important for the pre-pubertal adenogenesis [47–50]. For the post-pubertal adenogenesis, it is true that that low levels of estradiol might inhibit the gland growth. However, one unique phenotype in FOXL2^{OE} mice is the severely impaired penetration of the glands into the stroma. It is possible that without the appropriate penetration, the glands cannot elongate and branch further leading to a decrease in the number of glands. The increased collagen deposition may act as the physical obstacle of gland penetration, suggesting the importance of the endometrial stroma extracellular matrix in allowing normal uterine gland development.

Increased collagen deposition was also found in the Pgr^{cre} induced transforming growth factor-beta receptor 1 (TGFBR1) or smoothened (SMO) overexpression mouse models [51–53]. However, these studies did not exclude potential confounding factors from the ovary, so it is still unclear whether the uterine TGFBR1 and SMO are the major players. One study using FOXL2−/− male mice shows retarded cartilage and bone formation [54], suggesting a positive role for FOXL2 in regulation of cartilage formation. Our study presents direct evidence showing that uterine FOXL2 overexpression may increase collagen deposition. The inhibition of matrix metalloprotease signaling is mainly composed of matrix degradation-related genes. This signaling is enhanced in the 3-month-old FOXL2^{OE} uterine transcriptome indicating that FOXL2 can also increase collagen through inhibition of collagen degradation.

A previous study also reported a disorganized smooth muscle layer in Pgr^{cre} induced FOXL2 knockout mice [21] Together with our study, these observations indicate that appropriate FOXL2 levels are required for myometrium development. Similarly, either deletion or overexpression of TGFBR1 leads to disrupted smooth muscle layers suggesting the subtle roles of TGFβ pathways [53, 55]. Additionally, overexpressed TGFBR1 also reduced pre-pubertal adenogenesis [47]. Since the FOXL2-SMAD4 complexes act synergistically in the pituitary [12, 16], it is possible that FOXL2 also collaborated with the TGFβ pathways in the regulation of myometrium development.

Although the focus of this report was on the impact of FOXL2 overexpression on uterine function, there was an impact on ovulation observed. The ability of ovarian follicles to ovulate was blunted in the FOXL2^{OE} mice even after the mice were administered exogenous gonadotropins. Although the FOXL2 transgene could not be detected in non-stimulated mouse ovaries, consistent with the transient expression of PGR in the peri-ovulatory follicles [56], the Pgr^{cre} induced FOXL2 overexpression was detected in the peri-ovulatory follicles and corpus luteum in response to superovulation. It is well known that FOXL2 is mainly expressed in the granulosa cells of the ovary and is critical for the follicle development [57], but its functions in ovulation and corpus luteum remain unknown. In the human granulosa tumor cells, FOXL2 overexpression can alter the expression of molecules that is critical for ovulation, such as *IFNB1*, *IL12A*, and *PTGS2* [18], which may explain how FOXL2 overexpression dampens the ovulation. Since FOXL2 overexpression has been correlated with increased apoptosis in the granulosa tumor cells [58, 59], it is possible that FOXL2 overexpression also impaired granulosa cells from responding appropriately to the gonadotropin stimulus.

In addition to intrinsic actions of FOXL2 overexpression on the granulosa cells, it is clear that there was a disruption of the hypophyseal gonadal axis as evidence of the FOXL2^{OE} mice estrus cycle being in a constant state of diestrus. FOXL2 is identified as a critical regulator of the pituitary, in which the deletion of FOXL2 disrupts gonadotropin releasing that is necessary to stimulate appropriate follicular development and ovulation [11, 57]. FOXL2 is also detected in the hypothalamus and modifies *Ghrh* expression [54]. These data suggest a physiological role of FOXL2 in the pituitary and hypothalamus. The PGR expression in the pituitary and hypothalamus supports the potential of FOXL2 overexpression in the FOXL2^{OE} mice [60, 61]. However, the precise effects of FOXL2 overexpression on pituitary and hypothalamus require further investigation.

In addition to the structural alterations, the failure of the FOXL2^{OE} uterus to respond to the decidual cue indicates the functions of the uterus to support pregnancy were also impaired. Ovariectomy with exogenous hormone treatment eliminates the ovarian effects and indicates an intrinsic uterine defect. It is possible that the structural abnormality might lead to the function defects. The stratified epithelium may lose its ability to support the pregnancy. Previous studies identified that several mutant mouse models with epithelium stratification were infertile, such as $Pgr^{cre/+}Ctnnb1^{dd}$ mice [44], *Wnt7a*−/− [45] mice, and $Pgr^{cre/+}Sox17^{dd}$ mice [38]. However, since these mice exhibited multiple phenotypes, it is still too presumptuous to link the epithelial stratification with pregnancy failure. In contrast, the presence of functional glands is well known to be critical for uterine decidualization probably through Leukemia inhibitor factor (LIF) signaling [62–64]. The severely retarded adenogenesis in the FOXL2^{OE} uterus might be one of the major players in the failed decidualization. Besides, endometrial decidualization is promoted by mesenchymal-epithelial transition (MET) [65], whereas fibrosis is positively correlated with epithelial-mesenchymal transition [66]. Therefore, the exaggerated fibrosis observed in the FOXL2^{OE} uterine stroma might also blunt the decidualization through inhibiting the MET process.

In conclusion, our study demonstrates that the Pgr^{cre} induced *Foxl2* transgene expression can alter the uterine structures and functions, including adenogenesis, epithelium stratification, collagen deposition, and myometrial development. It provides a model to investigate the role of the stroma extracellular matrix in uterine gland development. It also provides new evidence of FOXL2 overexpression in regulating uterine and ovarian functions. Further studies are required to identify the underlying mechanism and the therapeutic potentials of FOXL2 in human.

Supplementary data

Supplementary data is available at *BIOLRE* online.

Acknowledgments

The authors acknowledge the Epigenomic and DNA Sequencing Core, The DNTP Clinical Pathology Core, the Integrative Bioinformatics Supportive

Group, the Fluorescence Microscopy and Imaging Center, and the Comparative Medicine Branch at NIEHS for their research support. The authors acknowledge Research in Reproduction Ligand Assay and Analysis Core, University of Virginia for serum analysis. The authors appreciated Dr Tianyuan Wang's consultation on bioinformatic analysis, Mr Linwood Koonce for mouse colony management, Ms Mita Ray for sharing the reagent, Ms Sylvia Hewitt for the constructive input on the paper, and Ms Janet DeMayo for the proofreading.

References

1. Ellsworth BS, Egashira N, Haller JL, Butts DL, Cocquet J, Clay CM, Osamura RY, Camper SA. FOXL2 in the pituitary: Molecular, genetic, and developmental analysis. *Mol Endocrinol* 2006; **20**:2796–2805.
2. Egashira N, Takekoshi S, Takei M, Teramoto A, Osamura RY. Expression of FOXL2 in human normal pituitaries and pituitary adenomas. *Mod Pathol* 2011; **24**:765–773.
3. Governini L, Carrarelli P, Rocha AL, Leo VD, Luddi A, Arcuri F, Piomboni P, Chapron C, Bilezikjian LM, Petraglia F. FOXL2 in human endometrium: Hyperexpressed in endometriosis. *Reprod Sci* 2014; **21**:1249–1255.
4. Brody JR, Histologic CGR. Morphometric, and Immunocytochemical analysis of Myometrial development in rats and mice. *1. Normal Development*. *American Journal of Anatomy* 1989; **186**:1–20.
5. Schmidt D, Ovitt CE, Anlag K, Fehsenfeld S, Gredsted L, Treier AC, Treier M. The murine winged-helix transcription factor Foxl2 is required for granulosa cell differentiation and ovary maintenance. *Development* 2004; **131**:933–942.
6. Uda M, Ottolenghi C, Deiana M, Kimber W, Forabosco A, Cao A, Schlessinger D, Pilia G. Foxl2 disruption causes mouse ovarian failure by pervasive blockage of follicle development. *Human Molecular Genetics* 2004; **13**:1171–1181.
7. Auguste A, Chassot AA, Gregoire EP, Renault L, Pannetier M, Treier M, Pailhoux E, Chaboissier MC. Loss of R-spondin1 and Foxl2 amplifies female-to-male sex reversal in XX mice. *Sex Dev* 2011; **5**:304–317.
8. Uhlenhaut NH, Jakob S, Anlag K, Eisenberger T, Sekido R, Kress J, Treier AC, Klugmann C, Klasen C, Holter NI, Riethmacher D, Schutz G et al. Somatic sex reprogramming of adult ovaries to testes by FOXL2 ablation. *Cell* 2009; **139**:1130–1142.
9. Nicol B, Grimm SA, Gruzdev A, Scott GJ, Ray MK, Yao HH. Genome-wide identification of FOXL2 binding and characterization of FOXL2 feminizing action in the fetal gonads. *Hum Mol Genet* 2018; **27**:4273–4287.
10. Tran S, Zhou X, Lafleur C, Calderon MJ, Ellsworth BS, Kimmins S, Boehm U, Treier M, Boerboom D, Bernard DJ. Impaired fertility and FSH synthesis in gonadotrope-specific Foxl2 knockout mice. *Mol Endocrinol* 2013; **27**:407–421.
11. Li Y, Schang G, Wang Y, Zhou X, Levasseur A, Boyer A, Deng CX, Treier M, Boehm U, Boerboom D, Bernard DJ. Conditional deletion of FOXL2 and SMAD4 in Gonadotropes of adult mice causes isolated FSH deficiency. *Endocrinology* 2018; **159**:2641–2655.
12. Lamba P, Wang Y, Tran S, Ouspenskaia T, Libasci V, Hebert TE, Miller GJ, Bernard DJ. Activin a regulates porcine follicle-stimulating hormone beta-subunit transcription via cooperative actions of SMADs and FOXL2. *Endocrinology* 2010; **151**:5456–5467.
13. Corpuz PS, Lindaman LL, Mellon PL, Coss D. FoxL2 is required for Activin induction of the mouse and human follicle-stimulating hormone beta-subunit genes. *Molecular Endocrinology* 2010; **24**: 1037–1051.
14. Tran S, Lamba P, Wang Y, Bernard DJ. SMADs and FOXL2 synergistically regulate murine FSHbeta transcription via a conserved proximal promoter element. *Mol Endocrinol* 2011; **25**:1170–1183.
15. Fortin J, Boehm U, Deng CX, Treier M, Bernard DJ. Follicle-stimulating hormone synthesis and fertility depend on SMAD4 and FOXL2. *FASEB J* 2014; **28**:3396–3410.
16. Liu XL, Meng YH, Wang JL, Yang BB, Zhang F, Tang SJ. FOXL2 suppresses proliferation, invasion and promotes apoptosis of cervical cancer cells. *International Journal of Clinical and Experimental Pathology* 2014; **7**:1534–1543.
17. Batista F, Vaiman D, Dausset J, Fellous M, Veitia RA. Potential targets of FOXL2, a transcription factor involved in craniofacial and follicular development, identified by transcriptomics. *Proceedings of the National Academy of Sciences of the United States of America* 2007; **104**:3330–3335.
18. Shah SP, Kobel M, Senz J, Morin RD, Clarke BA, Wiegand KC, Leung G, Zayed A, Mehl E, Kalloger SE, Sun M, Giuliany R et al. Mutation of FOXL2 in Granulosa-cell Tumors of the ovary. *New England Journal of Medicine* 2009; **360**:2719–2729.
19. Geiersbach KB, Jarboe EA, Jahromi MS, Baker CL, Paxton CN, Tripp SR, Schiffman JD. FOXL2 mutation and large-scale genomic imbalances in adult granulosa cell tumors of the ovary. *Cancer Genetics* 2011; **204**:596–602.
20. Eozenou C, Carvalho AV, Forde N, Giraud-Delville C, Gall L, Lonergan P, Auguste A, Charpigny G, Richard C, Pannetier M, Sandra O. FOXL2 is regulated during the bovine Estrous cycle and its expression in the endometrium is independent of Conceptus-derived interferon tau (vol 87, pg 1, 2012). *Biology of Reproduction* 2012; **87**.
21. Bellessort B, Bachelot A, Heude E, Alfama G, Fontaine A, Le Cardinal M, Treier M, Levi G. Role of Foxl2 in uterine maturation and function. *Human Molecular Genetics* 2015; **24**:3092–3103.
22. Elbaz M, Hadas R, Bilezikjian LM, Gershon E. Uterine Foxl2 regulates the adherence of the Trophectoderm cells to the endometrial epithelium. *Reprod Biol Endocrinol* 2018; **16**:12.
23. Soyal SM, Mukherjee A, Lee KY, Li J, Li H, DeMayo FJ, Lydon JP. Cre-mediated recombination in cell lineages that express the progesterone receptor. *Genesis* 2005; **41**:58–66.
24. Daikoku T, Ogawa Y, Terakawa J, Ogawa A, DeFalco T, Dey SK. Lactoferrin-iCre: A new mouse line to study uterine epithelial gene function. *Endocrinology* 2014; **155**:2718–2724.
25. Fedchenko N, Reifenrath J. Different approaches for interpretation and reporting of immunohistochemistry analysis results in the bone tissue - a review. *Diagn Pathol* 2014; **9**:221.
26. Huang DW, Sherman BT, Lempicki RA. Systematic and integrative analysis of large gene lists using DAVID bioinformatics resources. *Nature Protocols* 2009; **4**:44–57.
27. Huang DW, Sherman BT, Lempicki RA. Bioinformatics enrichment tools: Paths toward the comprehensive functional analysis of large gene lists. *Nucleic Acids Research* 2009; **37**:1–13.
28. Gray CA, Bartol FF, Tarleton BJ, Wiley AA, Johnson GA, Bazer FW, Spencer TE. Developmental biology of uterine glands. *Biology of Reproduction* 2001; **65**:1311–1323.
29. Bulun SE, Cheng YH, Pavone ME, Xue Q, Attar E, Trukhacheva E, Tokunaga H, Utsunomiya H, Yin P, Luo X, Lin Z, Imir G et al. Estrogen receptor-beta, estrogen receptor-alpha, and progesterone resistance in endometriosis. *Semin Reprod Med* 2010; **28**:36–43.
30. Akison LK, Robker RL. The critical roles of progesterone receptor (PGR) in ovulation, oocyte developmental competence and oviductal transport in mammalian reproduction. *Reprod Domest Anim* 2012; **47** Suppl 4:288–296.
31. Ramathal CY, Bagchi IC, Taylor RN, Bagchi MK. Endometrial decidualization: Of mice and men. *Semin Reprod Med* 2010; **28**:17–26.
32. Setiawan T, Buchanan D, Taylor JA, Young P, Lubahn DB, Cunha GR, Cooke PS. Role of stromal and epithelial estrogen receptors (ER) in uterine epithelial secretory protein production. *Biology of Reproduction* 1997; **56**:1–1.
33. Lydon JP, Demayo FJ, Funk CR, Mani SK, Hughes AR, Montgomery CA, Shyamala G, Conneely OM, Omalley BW. Mice lacking progesterone-receptor exhibit pleiotropic reproductive abnormalities. *Genes & Development* 1995; **9**:2266–2278.
34. Nanjappa MK, Medrano TI, March AG, Cooke PS. Neonatal uterine and vaginal cell proliferation and adenogenesis are independent of estrogen receptor 1 (ESR1) in the mouse. *Biol Reprod* 2015; **92**:78.
35. Stewart CA, Fisher SJ, Wang Y, Stewart MD, Hewitt SC, Rodriguez KF, Korach KS, Behringer RR. Uterine gland formation in mice is a continuous

process, requiring the ovary after puberty, but not after parturition. *Biology of Reproduction* 2011; **85**:954–964.
36. Burack E, Wolfe JM, Lansing W, Wright AW. The effect of age upon the connective tissue of the uterus, cervix. *and vagina of the rat. Cancer Research* 1941; **1**:227–235.
37. Bhartiya D, James K. Very small embryonic-like stem cells (VSELs) in adult mouse uterine perimetrium and myometrium. *Journal of Ovarian Research* 2017; **10**:1–12.
38. Wang X, Li X, Wang T, Wu SP, Jeong JW, Kim TH, Young SL, Lessey BA, Lanz RB, Lydon JP, DeMayo FJ. SOX17 regulates uterine epithelial-stromal cross-talk acting via a distal enhancer upstream of Ihh. *Nat Commun* 2018; **9**:4421.
39. Filant J, DeMayo FJ, Pru JK, Lydon JP, Spencer TE. Fibroblast growth factor receptor two (FGFR2) regulates uterine epithelial integrity and fertility in mice. *Biol Reprod* 2014; **90**:7.
40. Rubel CA, Wu SP, Lin L, Wang TY, Lanz RB, Li XL, Kommagani R, Franco HL, Camper SA, Tong Q, Jeong JW, Lydon JP et al. A Gata2-dependent transcription network regulates uterine progesterone responsiveness and endometrial function. *Cell Reports* 2016; **17**:1414–1425.
41. Iguchi T, Takase M, Takasugi N. Development of vaginal adenosis-like lesions and uterine epithelial stratification in mice exposed perinatally to diethylstilbestrol. *Proc Soc Exp Biol Med* 1986; **181**:59–65.
42. Kouzmenko AP, Takeyama K, Ito S, Furutani T, Sawatsubashi S, Maki A, Suzuki E, Kawasaki Y, Akiyama T, Tabata T, Kato S. Wnt/beta-catenin and estrogen signaling converge in vivo. *J Biol Chem* 2004; **279**:40255–40258.
43. Gao Y, Huang E, Zhang H, Wang J, Wu N, Chen X, Wang N, Wen S, Nan G, Deng F, Liao Z, Wu D et al. Crosstalk between Wnt/beta-catenin and estrogen receptor signaling synergistically promotes osteogenic differentiation of mesenchymal progenitor cells. *PLoS One* 2013; **8**:e82436.
44. Jeong JW, Lee HS, Franco HL, Broaddus RR, Taketo MM, Tsai SY, Lydon JP. DeMayo FJ. Beta-catenin mediates glandular formation and dysregulation of beta-catenin induces hyperplasia formation in the murine uterus. *Oncogene* 2009; **28**:31–40.
45. Miller C, Sassoon DA. Wnt-7a maintains appropriate uterine patterning during the development of the mouse female reproductive tract. *Development* 1998; **125**:3201–3211.
46. Gustin SE, Hogg K, Stringer JM, Rastetter RH, Pelosi E, Miles DC, Sinclair AH, Wilhelm D, Western PS. WNT/beta-catenin and p27/FOXL2 differentially regulate supporting cell proliferation in the developing ovary. *Developmental Biology* 2016; **412**:250–260.
47. Goad J, Ko YA, Kumar M, Syed SM, Tanwar PS. Differential Wnt signaling activity limits epithelial gland development to the anti-mesometrial side of the mouse uterus. *Developmental Biology* 2017; **423**:138–151.
48. Reardon SN, King ML, MacLean JA, Mann JL, DeMayo FJ, Lydon JP, Hayashi K. Cdh1 is essential for endometrial differentiation, gland development, and adult function in the mouse uterus. *Biology of Reproduction* 2012; **86**:1–10.
49. Dunlap KA, Filant J, Hayashi K, Rucker EB, Song G, Deng JM, Behringer RR, DeMayo FJ, Lydon J, Jeong JW, Spencer TE. Postnatal deletion of Wnt7a inhibits uterine gland morphogenesis and compromises adult fertility in mice. *Biology of Reproduction* 2011; **85**:386–396.
50. Mericskay M, Kitajewski J, Sassoon D. Wnt5a is required for proper epithelial-mesenchymal interactions in the uterus. *Development* 2004; **131**:2061–2072.
51. Ni N, Gao Y, Fang X, Melgar M, Vincent DF, Lydon JP, Bartholin L, Li Q. Glandular defects in the mouse uterus with sustained activation of TGF-beta signaling is associated with altered differentiation of endometrial stromal cells and formation of stromal compartment. *PLoS One* 2018; **13**:e0209417.
52. Franco HL, Lee KY, Rubel CA, Creighton CJ, White LD, Broaddus RR, Lewis MT, Lydon JP, Jeong JW, DeMayo FJ. Constitutive activation of smoothened leads to female infertility and altered uterine differentiation in the mouse. *Biol Reprod* 2010; **82**:991–999.
53. Gao Y, Duran S, Lydon JP, DeMayo FJ, Burghardt RC, Bayless KJ, Bartholin L, Li QL. Constitutive activation of transforming growth factor Beta receptor 1 in the mouse uterus impairs uterine morphology and function. *Biology of Reproduction* 2015; **92**:34.
54. Marongiu M, Marcia L, Pelosi E, Lovicu M, Deiana M, Zhang Y, Puddu A, Loi A, Uda M, Forabosco A, Schlessinger D, Crisponi L. FOXL2 modulates cartilage, skeletal development and IGF1-dependent growth in mice. *BMC Dev Biol* 2015; **15**:27.
55. Li QL, Martinez LM, Agno JE, Matzuk MM. Transforming growth factor beta receptor type 1 is essential for female reproductive tract development and function. *Biology of Reproduction* 2010; 88–88.
56. Robker RL, Akison LK, Russell DL. Control of oocyte release by progesterone receptor-regulated gene expression. *Nucl Recept Signal* 2009; **7**:e012.
57. Georges A, Auguste A, Bessiere L, Vanet A, Todeschini AL, Veitia RA. FOXL2: A central transcription factor of the ovary. *J Mol Endocrinol* 2014; **52**:R17–R33.
58. Cheng JC, Klausen C, Leung PC. Overexpression of wild-type but not C134W mutant FOXL2 enhances GnRH-induced cell apoptosis by increasing GnRH receptor expression in human granulosa cell tumors. *PLoS One* 2013; **8**:e55099.
59. Kim JH, Yoon S, Park M, Park HO, Ko JJ, Lee K, Bae J. Differential apoptotic activities of wild-type FOXL2 and the adult-type granulosa cell tumor-associated mutant FOXL2 (C134W). *Oncogene* 2011; **30**:1653–1663.
60. Sanchez-Criado JE, Trudgen K, Millan Y, Blanco A, Monterde J, Garrido-Gracia JC, Gordon A, Aguilar R, de Las Mulas JM, Ko C. Estrogen receptor (ESR) 2 partially offsets the absence of ESR1 in gonadotropes of pituitary-specific Esr1 knockout female mice. *Reproduction* 2012; **143**:549–558.
61. Gal A, Lin PC, Cacioppo JA, Hannon PR, Mahoney MM, Wolfe A, Fernandez-Valdivia R, Lydon JP, Elias CF, Ko C. Loss of fertility in the absence of progesterone receptor expression in Kisspeptin neurons of female mice. *PLoS One* 2016; **11**:e0159534.
62. Jeong JW, Kwak I, Lee KY, Kim TH, Large MJ, Stewart CL, Kaestner KH, Lydon JP, DeMayo FJ. Foxa2 is essential for mouse endometrial gland development and fertility. *Biology of Reproduction* 2010; **83**:396–403.
63. Kelleher AM, Peng W, Pru JK, Pru CA, DeMayo FJ, Spencer TE. Forkhead box a2 (FOXA2) is essential for uterine function and fertility. *Proc Natl Acad Sci U S A* 2017; **114**:E1018–E1026.
64. Filant J, Spencer TE. Endometrial glands are essential for blastocyst implantation and decidualization in the mouse uterus. *Biol Reprod* 2013; **88**:93.
65. Owusu-Akyaw A, Krishnamoorthy K, Goldsmith LT, Morelli SS. The role of mesenchymal-epithelial transition in endometrial function. *Hum Reprod Update* 2019; **25**:114–133.
66. Salton F, Volpe MC, Confalonieri M. Epithelial(−)Mesenchymal transition in the pathogenesis of idiopathic pulmonary fibrosis. *Medicina (Kaunas)* 2019; **55**:83.